

1 **CONSTRUCTION OF ULTRASOUND PHANTOMS WITH**
2 **WALL-LESS VESSELS USING 3D PRINTING**

3 Daniil I. Nikitichev^{1*}, PhD, A. Barburas¹, BSc, Kirstie McPherson², FRCA, Jean-Martial Mari^{1,3},
4 PhD, Simeon J. West², FRCA, and Adrien E. Desjardins¹, PhD

5 ¹Department of Medical Physics and Biomedical Engineering, Malet Place Engineering Building,
6 University College London, London WC1E 6BT, United Kingdom

7 ²University College Hospital, 235 Euston Road, London NW1 2BU, United Kingdom

8 ³Université de la Polynésie Française, Tahiti, French Polynesia

9 *Address correspondence to: Daniil Nikitichev, PhD, Gower Street, London, UK, WC1E
10 6BT, E-mail: d.nikitichev@ucl.ac.uk

11 Technical Innovation

12

13

14

15

16

17

18

19

20

21

22

23 **Summary.**

24 Ultrasound phantoms are invaluable as training tools for vascular access procedures. We
25 developed ultrasound phantoms with wall-less vessels using 3D printed chambers. Agar was used as a
26 soft-tissue mimicking material, and the wall-less vessels were created with rods that were retracted
27 after the agar was set. The chambers had integrated luer connectors to allow for fluid injections with
28 clinical syringes. Several variations on this design are presented, which include branched and stenotic
29 vessels. The results show that 3D printing can be well suited to the construction of wall-less
30 ultrasound phantoms, with designs that can be readily customised and shared electronically.

31 **Key words:** ultrasound phantom, vascular access; 3D printing; wall-less vessels; tissue-
32 mimicking material.

33

34

35 Ultrasound guidance is increasingly used to guide vascular access procedures, which include
36 peripheral venous, central venous, and arterial cannulation. Its usefulness depends significantly on the
37 skill of the operator, however. Proficiency with ultrasound-guided vascular access involves extensive
38 practice, as image interpretation and visualisation of the needle tip can be challenging. Ultrasound
39 phantoms are important for acquiring clinical skills before practising on live patients¹; it was recently
40 shown that clinicians who undertake simulation training on ultrasound guided vascular access achieve
41 higher success rates.^{2,3}

42 A wide range of commercial ultrasound phantoms have been developed for vascular access. They
43 tend to be expensive, with lifetimes limited by the tracks created by needle insertions. As such, they
44 are used sparingly in all but the most affluent clinical departments. Many custom phantoms have been
45 proposed as inexpensive alternatives to commercial phantoms. Lo et al., Kendall et al., Chatnler et al.,
46 Domenico et al., Terilinck et al.] [*Daniil, I don't think your current ref. 8 is relevant to this set of*
47 *references*] An aqueous gel such as agar can be advantageous as a tissue-mimicking material (TMM)
48 as it can readily be remade or melted to remove needle tracks. [Hocking et al.] [*Replace authors with*
49 *numbers*]

50 Many methods for creating vessels with flow in ultrasound phantoms have been proposed, with
51 or without vessel walls. Vessel walls can be mimicked with tubes positioned within the TMM [refs],
52 which can include simple cylindrical geometries [refs] and more realistic geometries created using 3D
53 printing moulds [refs] . They can be also created using tissue *ex vivo*¹⁰⁻¹² [also Bale-Glickman et al.
54 2003; KEber et al. 1992; Motomiya et al. 1984 – see references in Meagher 2007] at the expense of
55 experimental flexibility and repeatability. In wall-less phantoms, vessel walls are absent; a blood-
56 mimicking material (BMM) flows through a space created in the TMM. These types of phantoms can
57 be well suited to vascular access, as the vessel lumens can readily be accessed with needles and the
58 vessel boundaries can have realistic ultrasonic appearances.^{21,22} A simple construction method for
59 wall-less vessels involves retracting rods positioned into a TMM.²⁰ Wall-less vessels with more
60 realistic geometries can be created a lost-core method, which involves creating a solid, lumen-less
61 vessel, embedding it in a TMM, and subsequently melting away the solid vessel to create a space for
62 the BMM²³⁻²⁸ Despite their advantages, wall-less phantoms are not widespread in clinical practice.

63 Their limited adoption at present may be due in large part to the inconvenience and the mechanical
64 workshop resources required to create chambers with ports with which wall-vessels can be created.

65 In this study, ultrasound phantoms with 3D printed chambers and different wall-less vessel
66 geometries were developed for vascular access. Variations in the surface quality of the chambers,
67 which can arise from different chamber geometries and the use of different printers, were explored.

68 **Materials and Methods**

69 Each ultrasound phantom comprised a 3D printed rectangular chamber in which agar was poured
70 as a soft-tissue mimicking material (Figure 1).³⁰ The dimensions of this chamber (100 × 100 mm; 60
71 mm height) were compatible with typical ultrasound imaging probes and they allowed for in-plane
72 and out-of-plane needle insertions. Wall-less vessels were created by placing rods in the chamber
73 before the agar was poured, and removing them after the agar was set (Figure 2a-e). Within the
74 chamber, the rods were fixed in angle with small support tubes printed in the sides of the box (star on
75 Figure 1). Since the diameters of the wall-less vessels were significantly larger than those of the
76 lumens of the luer connectors, the support tubes extended out of the chamber but not within the luer
77 connectors. On one side of the chamber, the ends of the support tubes had luer connectors that
78 allowed for fluid to be injected through the vessels after the rods were removed (Figure 2f). Support
79 tubes on the other side of the box could be connected to tubing (inner diameter: 8.5 mm) to receive
80 fluid from the vessels. The support tubes protruded slightly inside the chamber to accommodate
81 shrinkage of the agar after setting. A small tray accommodated fluid outflow when tubes on the side
82 of the box opposite the luer connectors were not connected to tubing. Printed caps for the luer
83 connectors were used to prevent the agar from flowing out of the chamber before it was set.

84 Three ultrasound phantoms with wall-less vessels were created. The first phantom comprised two
85 parallel wall-less vessels with different diameters (12 mm and 6 mm) that were made using solid rods.
86 These diameters were chosen to correspond to a large artery/vein pair. In one variation of this
87 phantom, the vessels were horizontal; in another, they were vertically angled at 20 degrees. With both
88 variations, polytetrafluoroethylene (PTFE rods, DirectPlastics, Sheffield, UK) was chosen as the
89 material for the rods to minimise adhesion with the agar. The second phantom comprised a branched

90 vessel, which was created with two rods. Each of these rods was 3D printed, as a combination of two
91 hemispherical parts (Figure 3a). The first rod was positioned horizontally in the chamber; the second
92 was partially inserted into a groove in the first and vertically angled at 20 degrees (Figure 3b). The
93 two-part rod design stemmed from the need for smooth surfaces to minimise adhesion to the agar and
94 thereby to create smooth vessels when retracted, and from the observation that 3D printed surfaces
95 that were in contact with support material during the printing process tended to be significantly less
96 smooth than those that are not. Each hemispherical part was printed with its curved surface upward,
97 so that it was not in contact with support material. The third phantom comprised a stenotic vessel that
98 was created with two rods, similar to one that was previously demonstrated by Qian et al. [31]. These
99 rods were 3D printed in the same manner as they were for the second phantom, except that one rod
100 had a small cavity in which the other could be positioned (Figure 3c). The diameter of these rods was
101 4 mm along a distance of 20 mm (centred at the point of apposition) and 6.2 mm elsewhere; the
102 narrowing mimicked a stenosis when the rods were retracted.

103 The chamber was designed using two freely available software programs: Blender (Stichting
104 Blender Foundation, Amsterdam, the Netherlands), and FreeCAD (Juergen Riegel, Werner Mayer,
105 Yorik van Havre, OpenSource, freecad.com). The 3D printing files (STL format) are included as
106 supplemental materials. Two different printers were used; each required approximately 240 g of build
107 material and 80 g of support material. The first printer, which will be denoted Printer 1, was an
108 additive polymer resin printer (Objet30 Pro, Stratasys, Eden Prairie, Minnesota) using a rigid opaque
109 white or blue material with a gloss finish (VeroWhitePlus RGD835 or VeroBlue, accuracy <0.1mm).
110 The second (Printer 2) was a an extruded thermoplastic polymer printer (Ultimaker2, Ultimaker,
111 Chorley Lancashire, UK) using a filament material (PolyMax, Polymakr, Changshu, China, accuracy
112 >0.1mm). The printing costs varied significantly with the printer: £44 GBPper phantom for Printer 1
113 and £3 GBP per phantom for Printer 2. By comparison, the costs of commercial vascular access
114 phantoms are typically in excess of £1000.

115 The agar (A7002; Sigma-Aldrich, St. Louis, Missouri) was dissolved in hot water (> 90°C)
116 outside the chamber to bring it above its melting point (85 °C), with a concentration of 5.5% by
117 weight. This concentration is similar to those previously used.^{6,32}. A hot plate was found to be useful

118 to maintain the high temperature during dissolution; without it, rapid mixing is required and
119 consequently there is a risk of introducing bubbles. It was found that the use of a degassing chamber
120 for 5 minutes was useful to remove residual bubbles.³⁴ After mixing, the melted agar solution was
121 cooled to a temperature in the range of 50 to 55 °C, which was below the range in which the 3D
122 printing material distorts and above the gel point of agar. The solution was poured into the 3D printed
123 chamber and the phantom was placed in a refrigerator (~4 °C) for 24 hours prior to removing the
124 rods.

125 The phantom was imaged with a linear array transducer probe (L14-5/38; SonixMDP, Analogic
126 Ultrasound, Richmond, BC, Canada). Prior to imaging, the vessels were filled with water using two
127 10 mL syringes connected directly to the chamber. In-plane and out-of-plane needle insertions were
128 performed using ultrasound imaging guidance with an injection needle (18 G, Terumo).

129 **Results**

130 The surface quality and the mechanical robustness of the 3D printed chambers depended
131 significantly on the printing process that was used (Figure 1). Both chambers were waterproof and
132 could withstand accidental needle pricks. Printer 1 produced a chamber with a much smoother surface
133 and its output had superior resolution and mechanical integrity. A prominent difference between the
134 printer outputs was found between the luer connectors: those obtained with Printer 2 readily broke
135 with regular usage and the grooves were incompletely delineated (Figure 3 insets). Manual removal of
136 the printing support material, which is required before the chamber can be used, could be achieved
137 more easily when Printer 1 was used.

138 As seen with ultrasound imaging, wall-less vessels in all three phantoms had circular cross-
139 sections throughout their length (Figure 4). Needles could readily be inserted into the agar and into
140 the vessels. The resistance to insertion was less than that typically encountered in vascular access
141 procedures, however, and resistance was not encountered during transitions from agar to the vessel
142 lumens. Needles were readily visualised on ultrasound, with out-of-plane (Figure 4a) and in-plane
143 (Figure 4b) insertions. Residual needle tracks were apparent, but these could be removed by remaking
144 the phantom.

145 The agar surrounding these vessels had a homogeneous speckled appearance on ultrasound,
146 similar to that of tissue. At the surface of the phantoms, the agar was sufficiently rigid to resist
147 deformation by the ultrasound imaging probe with light pressure consistent with clinical practice, but
148 care was needed to ensure integrity of the surface. The vessels maintained their shape during
149 injections of water, without fluid leaks. In the branched vessel phantom, the thin agar at the
150 bifurcation point (Figure 4c) was prone to damage during injections. With the stenotic phantom, the
151 variation in vessel diameter was clearly apparent (Figure 4d), and the stenotic region presented as
152 uniform along its length with smooth walls that tapered on either side to wider regions.

153 **Discussion**

154 In this study, the use of 3D printing for the manufacturing of agar wall-less vascular phantoms
155 was explored with three different vessel geometries. The use of 3D printing has two main advantages
156 that make it compelling for use in clinical environments. First, it makes the creation of chamber
157 geometries with multiple inset tubular structures and fabrication of luer connectors straightforward,
158 even in the absence of mechanical workshop resources. Second, the design files can readily be shared
159 electronically and modified to accommodate different types of training.

160 The phantom chamber design lends itself to several variations that could provide different
161 functionalities. For instance, a pump that provides pulsatile flow and blood mimicking fluid could be
162 used for practising with Doppler ultrasound imaging, as considered in a previous study.^{31, 34} Wall-less
163 vessel phantoms have been found to be inferior to those with vessel-mimicking material¹⁵, and so
164 testing would be required before this method of fabrication could be recommended.

165 A homogenous agar region surrounding the wall-less vessels is attractive from the standpoint of
166 simplicity, but the use of different materials could allow for inhomogeneities that increase realism. As
167 a variation on the phantom in this study, different layers of aqueous gels could be formed by pouring
168 melted gel on top of a set gel layer; the resulting layers could have additions with different
169 concentrations to control their ultrasonic properties. For instance, gelatine, as an aqueous gel, could
170 include a combination of graphite particles for control of ultrasound attenuation and alcohol for
171 control of the speed of sound.^{30,35} Ultimately, 3D printing could be used to deposit soft-tissue

172 mimicking materials directly with 3D printing, which could lead to printing complex structures such
173 as the brachial plexus and even to creating patient-specific phantoms based on segmented pre-
174 procedural images. An analogous approach was explored for creating optical phantoms³⁶.

175 This study demonstrated that 3D printing is well suited to the creation of wall-less vascular
176 ultrasound phantoms that include branched and stenotic vessels. The approach taken in this paper is
177 particularly well suited to efficient, low-cost vascular phantoms for clinical training.

178 **Acknowledgements**

179 The authors gratefully acknowledge funding from European Starting Grant 310970 MOPHIM and
180 from an Engineering and Physical Research Council (EPSRC) Vacation Bursary for A. Barburas, and
181 helpful discussions with Dr. Wenfeng Xia.

182 **References**

- 183 1. McGaghie WC, Issenberg SB, Petrusa ER, Scalese RJ. A critical review of simulation-based
184 medical education research: 2003-2009. *Med. Educ.* 2010; 44: 50–63.
- 185 2. Blaivas M, Adhikari S. An unseen danger: frequency of posterior vessel wall penetration by
186 needles during attempts to place internal jugular vein central catheters using ultrasound
187 guidance. *Crit. Care Med.* 2009; 37: 2345–2349.
- 188 3. Bohlega S, Mclean DR. Hemiplegia caused by inadvertent intra-carotid infusion of total
189 parenteral nutrition. *Crit. Care Med.* 1997; 99: 217–219.
- 190 4. Lo MD., Ackley SH., Solari P. Homemade ultrasound phantom for teaching identification of
191 superficial soft tissue abscess. *Emerg. Med. J.* 2012; 29:738-741.
- 192 5. Kendall JL., Faragher JP. Ultrasound-guided central venous access: a homemade phantom for
193 simulation. *Canadian J. of Emer. Med.* 2007; 9:371-373.
- 194 6. Chantler J, Gale L, Weldon O. A reusable ultrasound phantom. *Anaesthesia* 2004; 59: 1145–
195 1146.
- 196 7. Domenico SD, Santori G, Procile E, Licausi M, Centanaro M, Valente U. Inexpensive
197 homemade models for ultrasound-guided vein cannulation training. *J. of Clinic. Anesth.* 2007;
198 19:491-496.
- 199 8. Hocking G, Hebard S, Mitchell CH. A Review of the Benefits and Pitfalls of Phantoms in
200 Ultrasound-Guided Regional Anesthesia. *Reg. Anesth. Pain Med.* 2011; 36: 162–170.
- 201 9. Teirlinck CJ, Bezemer RA, Kollmann C, Lubbers J, Hoskins PR, Ramnarine KV, Fish P,
202 Fredeldt KE, Schaarschmidt UG, Development of an example flow test object and comparison
203 of five of these test objects, constructed in various laboratories. *Ultrasonics* 1998; 36: 653-660.

- 204 10. Greaby R, Zderic V, Vaezy S. Pulsatile flow phantom for ultrasound image-guided HIFU
205 treatment of vascular injuries. *Ultrasound in Med. and Biol.* 2007; 33: 1269-1276.
- 206 11. Dabrowski W, Dunmore-Buyze J, Rankin RN, Holdsworth DW, Fenster A. A real vessel
207 phantom for imaging experimentation. *Med. Phys.* 1997; 24: 687-693.
- 208 12. Dabrowski W, Dunmore-Buyze J, Cardinal HN, Fenster A. A real vessel phantom for flow
209 imaging: 3D Doppler ultrasound of steady flow. *Ultrasound Med. Biol.* 2001; 27: 135-141.
- 210 13. Dineley J, Meagher S, Poepping TL, McDicken WN, Hoskins PR. Design and characterisation
211 of a wall motion phantom. *Ultrasound in Med. and Biol.* 2006; 32: 1349-1357.
- 212 14. Qian M, Niu L, Wong KKL, Abbott D, Zhou Q, Zheng H. Pulsatile flow characterization in a
213 vessel phantom with elastic wall using ultrasonic particle image velocimetry technique: The
214 impact of vessel stiffness on flow dynamics. *IEEE Tran. Biomed. Eng.* 2014, 61: 2444-2450.
- 215 15. King DM, Moran CM, McNamara JD, Fagan A, Browne JE. Development of a vessel-
216 mimicking material for use in anatomically realistic doppler flow phantoms. *Ultrasound in*
217 *Med. and Biol.* 2011; 37: 813-826.
- 218 16. King DM, Ring M, Moran CM, Browne JE. Development of a range of anatomically realistic
219 renal artery flow phantoms. *Ultrasound in Med. and Biol.* 2010; 36: 1135-1144.
- 220 17. Surrey KJM, Austin HJB, Fenster A, Peters TM. Poly(vinyl alcohol) cryogel phantoms for use
221 in ultrasound and MR imaging. *Phys. Med. Biol.* 2004; 49: 5529-5546.
- 222 18. Poepping TL, Nikolov HN, Thorne ML, Holdsworth DW. A thin-walled carotid vessel
223 phantom for Doppler ultrasound flow studies. *Ultrasound in Med. and Biol.* 2004; 30: 1067-
224 1078.

- 225 19 Bale-Glickman J, Selby K, Saloner D, Savas O. Experimental flow studies in exact-replica
226 phantoms of atherosclerotic carotid bifucations under steady input conditions. *J. Biomech.*
227 *Eng.* 2003; 125: 38-48.
- 228 20. Guo Z, Fenster A. Three-dimensional power Doppler imaging: A phantom study to quantify
229 vessel stenosis. *Ultrasound Med. Biol.* 1996; 22: 1059-1069.
- 230 21. Rickey DW, Picot PA, Christopher DA, Fenster A. A wall-less vessel phantom for Doppler
231 ultrasound studies. *Ultrasound Med. Biol.* 1995; 21: 1163–1176.
- 232 22. Ramnarine KV, Anderson T, Hoskins PR. Construction and geometric stability of
233 physiological flow rate wall-less stenosis phantoms. *Ultrasound Med. Biol.* 2001; 27: 245–
234 250.
- 235 23. Smith RF, Rutt BK, Holdsworth DW. Anthropomorphic carotid bifurcation phantom for MRI
236 applications. *J. Magn. Reson. Imaging* 1999; 10: 533-544.
- 237 24. Watts DM, Sutcliffe CJ, Morgan RH, et. al. Anatomical flow phantoms of the nonplanar
238 carotid bifurcation. Part I: computer-aided design and fabrication. *Ultrasound Med. Biol.* 2007;
239 33: 296-302.
- 240 25. Meagher S, Poepping TL, Ramnarine KV, et. al. Anatomical flow phantoms of the nonplanar
241 carotid bifurcation. Part II: Experimental validation with Doppler ultrasound. *Ultrasound Med.*
242 *Biol.* 2007; 33: 303-310.
- 243 26. Poepping TL, Nikolov HN, Rankin RN, et. al. An *in vitro* system for Doppler ultrasound flow
244 studies in the stenosed carotid artery bifurcation. *Ultrasound Med. Biol.* 2002; 28:495-506.
- 245 27 Cloutier G, Soulez G, Qanadli SD, et. al. A multimodality vascular imaging phantom with
246 fiducial markers visible in DSA, CTA, MRA, and ultrasound. *Med. Phys.* 2004; 31: 1424-
247 1433.

- 248 28 Frayne R, Gowman LM, Rickey DW, et. al. A geometrically accurate vascular phantom for
249 comparative studies of x-ray, ultrasound, and magnetic resonance vascular imaging:
250 construction and geometrical verification. *Med. Phys.* 1993; 20: 415-425.
- 251 29 Kenwright D, Laverick N, Anderson T, et. al. Wall-less flow phantom for high-frequency
252 ultrasound applicatons. *Ultrasound Med. Biol.* 2015; 41: 890-897.
- 253 30. Madsen EL, Zagrebski JA, Banjavie RA, Jutila RE. Tissue mimicking materials for ultrasound
254 phantoms. *Mecical Phys.* 1978; 5: 391–394.
- 255
- 256 31. Qian M, Song R, Niu L, et. al. Two-dimensional flow study in a stenotic artery phantom using
257 ultrasonic particle image velocimetry. Proc. of Annual Inter. Conf. IEEE in Med. and Biol.
258 2011, 563-566.
- 259 32. West SJ, Mari J-M, Khan A, et al. Development of an ultrasound phantom for spinal injections
260 with 3-dimensional printing. *Reg. Anesth. Pain Med.* 2014; 39: 429–33.
- 261 33. Nicholson RA, Crofton M. Training phantom for ultrasound guided biopsy. *Br. J. Radiol.*
262 1997; 70: 192–194.
- 263 34. Lai SSM, Yiu BYS, Poon AKK, Yu ACH. Design of anthropomorphic flow phantoms based
264 on rapid prototyping of compliant vessel geometries. *Ultrasound Med. Biol.* 2013; 39: 1654–
265
- 266 35. Culjat MO, Goldenberg D, Tewari P, Singh RS. A review of tissue substitutes for ultrasound
267 imaging. *Ultrasound Med. Biol.* 2010; 36: 861–73.
- 268 36. Wang J, Coburn J, Liang C-P, et al. Characterization and application of 3D-printed phantoms
269 for biophotonic imaging. in *Proc. SPIE 8719, Smart Biomed. Physiol. Sens. Technol. X* 2013;
270 8719: 87190Y.

271

272

273

274

275

276

277

278 **Figure Captions**

279 **Figure 1.** Chamber for phantom with two parallel vessels: **(a)** software rendering; **(b)** printed with
280 Printer 2; **(c)** printed with Printer 1. The insets provide a close-up of one of the luer connectors
281 (arrow). * denotes support tubes.

282

283 **Figure 2.** Phantom fabrication using the 3D printed chamber.

284

285 **Figure 3.** Design of the vessel rods for the development of **(a)** the wall-less phantom; **(b)** the
286 branching phantom; **(c)** the stenotic phantom (outer diameters: $D1 = 4$ mm; $D2 = 6.2$ mm).

287

288 **Figure 4.** Wall-less vessel phantoms imaged with a linear array transducer probe. During imaging, the
289 vessels were filled with water using two 10 mL syringes connected to the chamber. Needle insertions
290 into the parallel vessel phantom were performed **(a)** out-of-plane and **(b)** in-plane; the needle tip was
291 visible in both views (dashed circles). The branching phantom **(c)** and the stenotic phantom **(d)** are

292 imaged in cross-section; in the latter, the boundaries of the narrow diameter region are shown with
293 arrows.

294

295

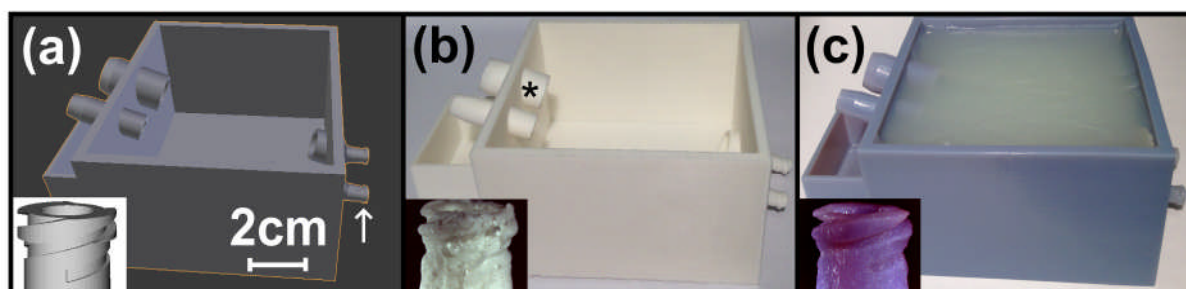
296

297

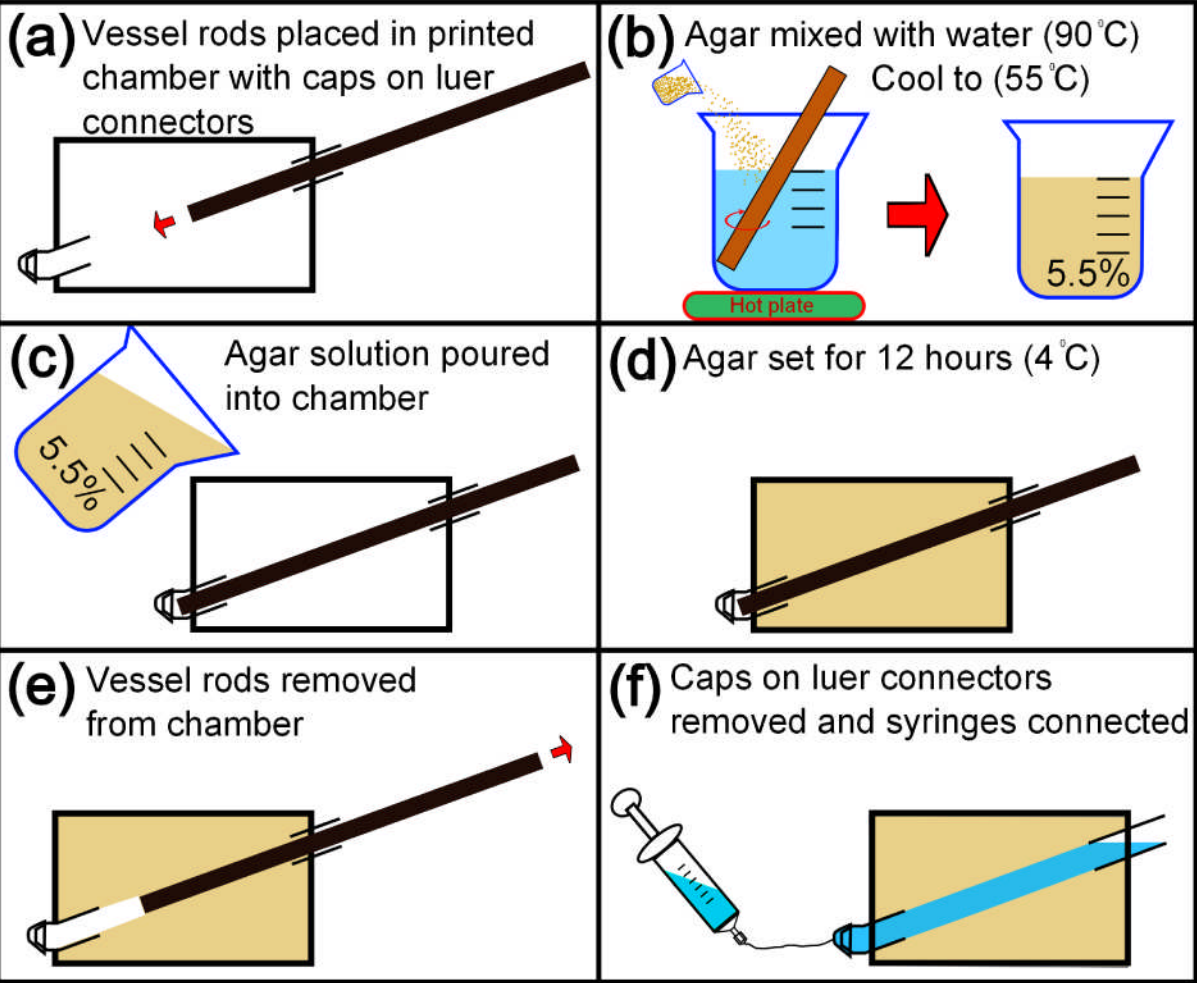
298

299

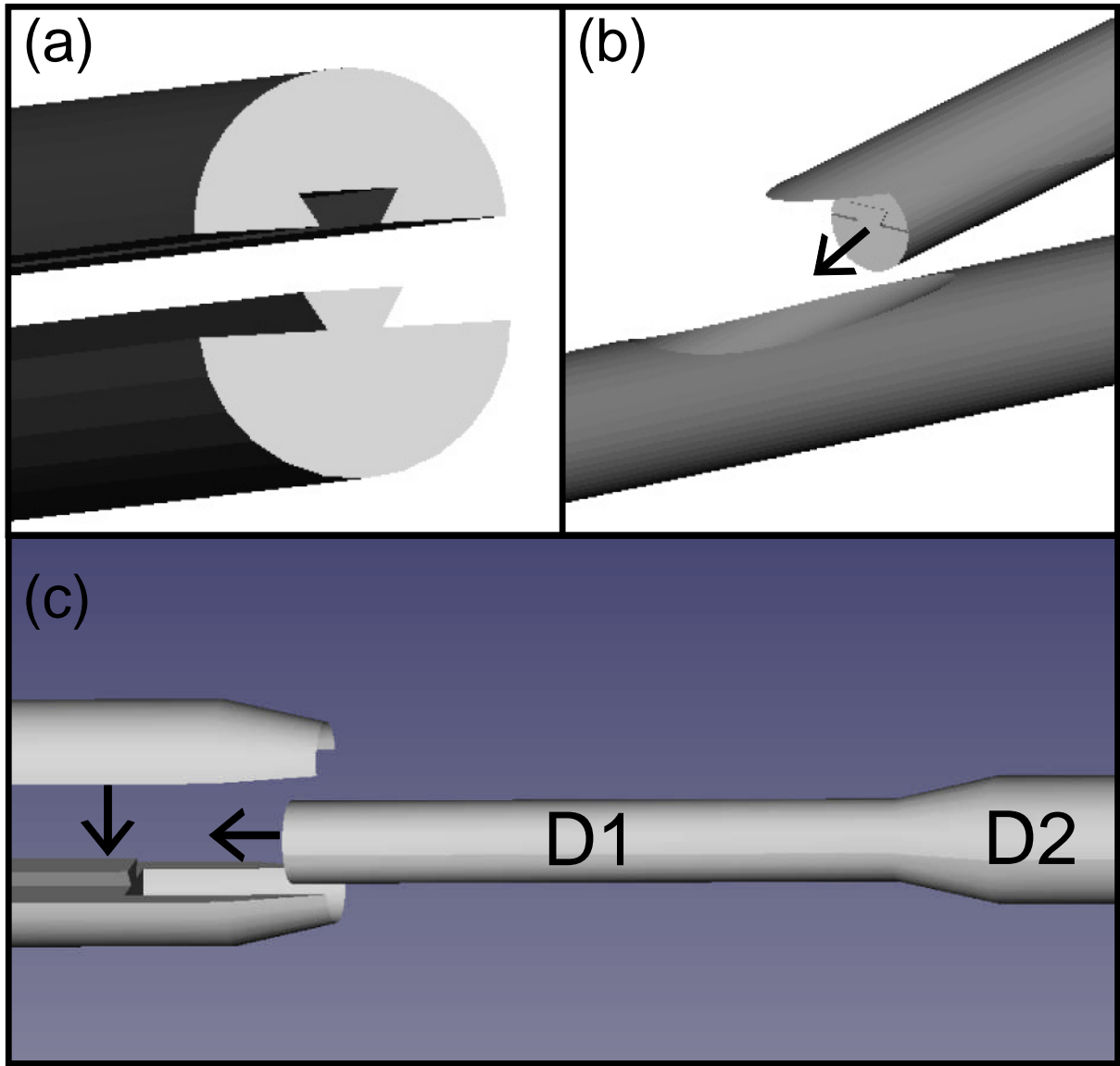
300



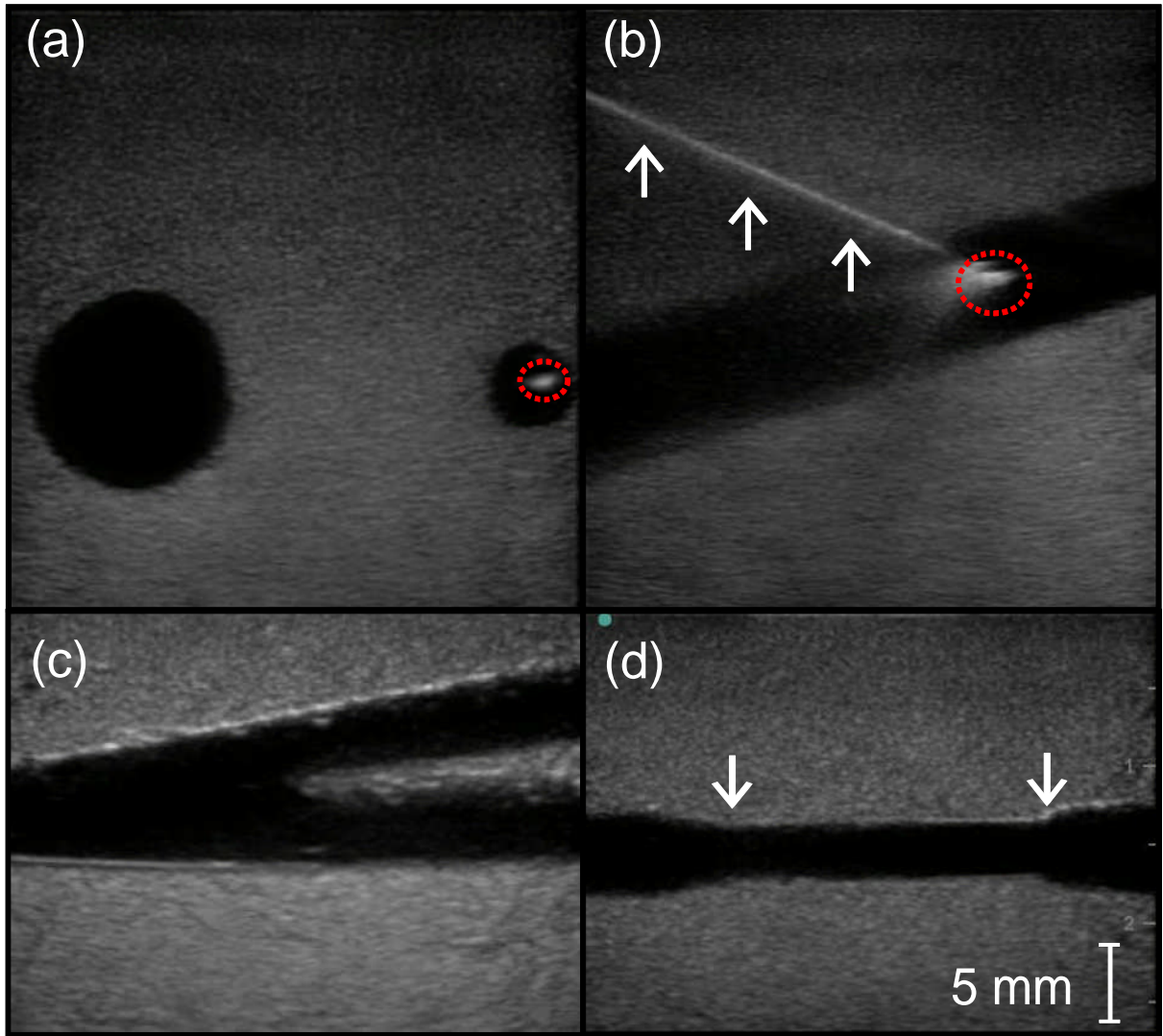
301



302



303



304